PS-2-8

Extended Abstracts of the 2012 International Conference on Solid State Devices and Materials, Kyoto, 2012, pp56-57

Evaluation of Threshold Current Density in Interconnect with Reservoir Structure Using Numerical Modeling of Electromigration Damage

Kazuhiko Sasagawa and Tahahiro Yanagi

Department of Intelligent Machines and System Engineering,
Hirosaki University
3 Bunkyo-cho, Hirosaki 036-8561, Japan
Phone&Fax: +81-172-39-3675
E-mail: sasagawa@cc.hirosaki-u.ac.jp

1. Introduction

Reservoir structures have overhang from via connection, and usually located on both anode and cathode ends as shown Fig.1. It is known that reservoir structure gives delay of electromigration(EM) failure in multilevel interconnection by increasing margin of critical void length.

On the other hand, it is known that there is a threshold current density j_{th} of EM damage in the via-connected line. Namely, current density below j_{th} does not cause drift damage. However, the effect of reservoir on j_{th} does not seem to be clarified.

Some research groups have developed evaluation method of j_{th}[1]. The threshold current density is also evaluated by numerical simulation. The building-up process of atomic density distribution in the line is simulated. And this simulation is based on governing parameter for EM damage in polycrystalline line AFD^{*}_{gen}. Sasagawa et al. evaluated j_{th} of several kinds of two-dimensional interconnect tree [2]. And they showed increase in j_{th} of angled line in comparison of straight line.

In this study, we modify the numerical models for evaluation of interconnect tree to apply to evaluation of reservoir structure. And we evaluate j_{th} of several kinds of via-connected line with reservoir by the numerical simulation. From the evaluation results, reservoir effects on the threshold current density are discussed.

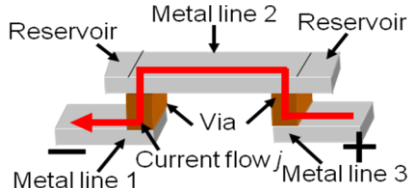

Fig. 1 Multilayer interconnection with reservoir struc

2. Simulation method

The governing parameter for EM damage is used for constructing the numerical simulation [3]. The parameter is given the formulation of divergence of atomic flux due to EM. The atomic flux, **J** is represented by Eq. 1.

$$|\mathbf{J}| = \frac{ND_0}{kT}\exp\left\{-\frac{Q_{gb}+\kappa\Omega(N-N_T)/N_0-\sigma_T\Omega}{kT}\right\}\left(Z^{*}e\rho j^{*}-\frac{\kappa\Omega}{N_0}\frac{\partial N}{\partial l}\right) \quad (1)$$

where **J** is the atomic flux vector, N atomic density, D_0 a prefactor, k Boltzmann's constant, T the absolute temperature, Q net activation energy for atomic diffusion, κ the constant relating the change in stress with the change in atomic density under restriction by passivation, N_T the atomic density under tensile thermal stress σ_T, N_0 the atomic density at a reference condition, Ω the atomic volume, Z^* the effective valence and e the electronic charge. ρ is the temperature-dependent resistivity. Symbols j^* and $\partial N/\partial l$ are the components of the current density vector and atomic density gradient in the direction of **J**, respectively.

We assumed grain boundary diffusion as dominant diffusion mechanism in the simulation, because wide Cu lines covered with Ta liner were supposed. According to literature [4][5], in wide Cu interconnects, grain boundaries become preferential EM paths. Sasagawa et al introduced a grain texture model for calculating atomic flux divergence [6]. So we used the governing parameter for EM damage based on the model even for copper lines.

Considering atoms going in and out at a unit rectangle, atomic flux divergence in polycrystalline line is formulated as given in Eq. 2.

$$\begin{aligned}
AFD^{*}_{gb\theta} &= C^{*}_{gb} N \frac{4}{\sqrt{3}d^2}\frac{1}{T}\exp\left\{-\frac{Q_{gb}+\kappa\Omega(N-N_T)/N_0-\sigma_T\Omega}{kT}\right\}\times \\
&\left\langle \sqrt{3}\Delta\varphi\left\{(j_x\cos\theta + j_y\sin\theta)Z^{*}e\rho - \frac{\kappa\Omega}{N_0}\left(\frac{\partial N}{\partial x}\cos\theta + \frac{\partial N}{\partial y}\sin\theta\right)\right\}\right. \\
&-\frac{d}{2}\Delta\varphi\left\{\left(\frac{\partial j_x}{\partial x}-\frac{\partial j_y}{\partial y}\right)Z^{*}e\rho\cos 2\theta - \frac{\kappa\Omega}{N_0}\left(\frac{\partial^2 N}{\partial x^2}-\frac{\partial^2 N}{\partial y^2}\right)\cos 2\theta\right. \\
&\left.+\left(\frac{\partial j_x}{\partial y}+\frac{\partial j_y}{\partial x}\right)Z^{*}e\rho\sin 2\theta - 2\frac{\kappa\Omega}{N_0}\frac{\partial^2 N}{\partial x\partial y}\sin 2\theta\right\} - \frac{\sqrt{3}}{4}d\frac{\kappa\Omega}{N_0}\left(\frac{\partial^2 N}{\partial x^2}+\frac{\partial^2 N}{\partial y^2}\right) \\
&-\frac{\kappa\Omega/N_0}{kT}\left[\frac{\sqrt{3}}{4}d\left\{Z^{*}e\rho\left(j_x\frac{\partial N}{\partial x}+j_y\frac{\partial N}{\partial y}\right)-\frac{\kappa\Omega}{N_0}\left(\frac{\partial N}{\partial x}\frac{\partial N}{\partial x}+\frac{\partial N}{\partial y}\frac{\partial N}{\partial y}\right)\right\}\right. \\
&\left.-\frac{d}{2}\Delta\varphi\left\{Z^{*}e\rho\left(j_y\frac{\partial N}{\partial x}+j_x\frac{\partial N}{\partial y}\right)-2\frac{\kappa\Omega}{N_0}\frac{\partial N}{\partial x}\frac{\partial N}{\partial y}\right\}\sin 2\theta\right] \\
&+\frac{\sqrt{3}d}{4T}\left\{\frac{Q_{gb}+\kappa\Omega(N-N_T)/N_0-\sigma_T\Omega}{kT}-1\right\} \\
&\left.\left\{Z^{*}e\rho\left(j_x\frac{\partial T}{\partial x}+j_y\frac{\partial T}{\partial y}\right)-\frac{\kappa\Omega}{N_0}\left(\frac{\partial N}{\partial x}\frac{\partial T}{\partial x}+\frac{\partial N}{\partial y}\frac{\partial T}{\partial y}\right)\right\}\right\rangle
\end{aligned} \quad (2)$$

At line ends, boundary condition with respect to atomic flow has to be given to the formulation of the parameter at line ends. Namely, there is no coming-in at cathode end and

no going-out at anode one. The boundary condition can be expressed by possible zero flux within the microstructure unit being assigned to each unit angle θ-range [7].

The computational procedure is shown in Fig.2. At first, the distributions of current density and temperature are calculated by 2-dimensional FE analysis. The governing parameters are calculated in each element from the analysis results and the film characteristics. Next, the atomic density is calculated based on the value of the governing parameter. By the repetitive calculation, the atomic density distribution in the line evolves with time. The repetitive calculation is performed until the atomic density reaches a critical atomic density for damage initiation or until the atomic density distribution holds a steady state.

3. Evaluation

We evaluated three line structures as shown in Fig.3. Sample 1 has no reservoir at both ends of line. In Sample 2, a reservoir locates only on the cathode via. In Sample 3, two reservoirs locate on both vias. This structure is typical.

After the simulation with small current density below the threshold, we got steady state distribution of atomic density. The smallest value of the atomic density N^* in all elements at steady state is plotted against supposed current density j. From an intersection point of the line of the smallest atomic density N^* and the critical density indicated by dotted line, the threshold current density is evaluated.

4. Results and discussion

As the result, in Sample 2, j_{th} became larger than those in Sample 1 and 3 as shown in Fig.4. We can explain the change in j_{th} from viewpoint of atomic density distribution as shown in Fig.5. In Sample 1 and 2, under input current density is the same. According to Eq. (1), if current density is the same, driving force of EM is same. So at steady state, the slope of atomic density corresponds each other. On the other hand, current density in reservoir is almost zero, and there is not driving force of EM. So at steady state, the slope in reservoir is almost horizontally. According to law conservation of mass, atomic density distribution in Sample 2 must be shifted upward globally from distribution in Sample 1.

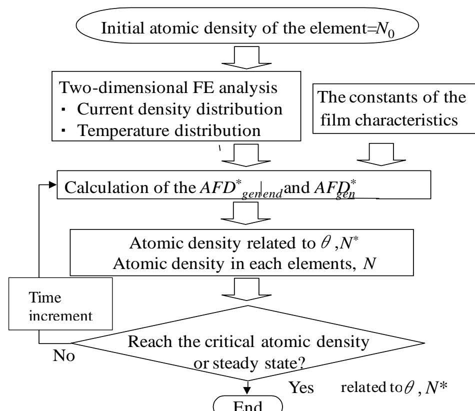

Fig.2 Computational procedure for evaluation of the threshold current density

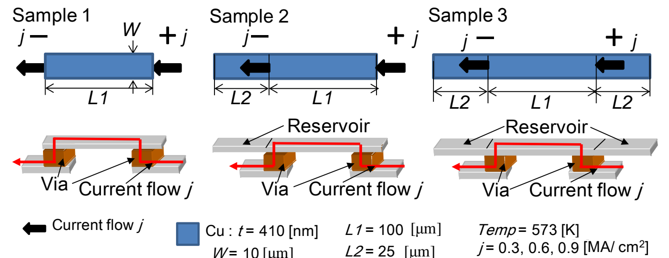

Fig.3 The dimension and structure of the supposed lines

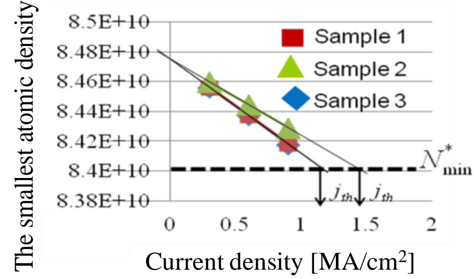

Fig.4 Result of threshold current density in simulation

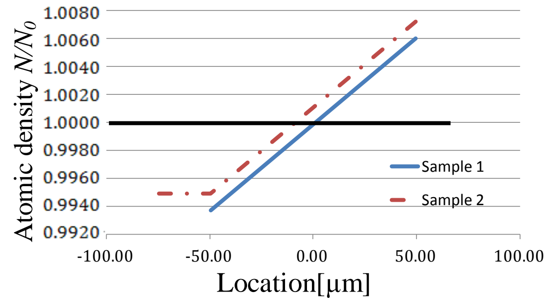

Fig.5 Distribution of atomic density N/N_0

5. Conclusions

AFD^*_{gen} -based evaluation of j_{th} was carried out and the modified numerical models ware applied to numerical simulation of atomic density distribution. We found that if a reservoir is located only on the cathode side, the threshold current density of EM damage is increased. And we concluded that this phenomenon is caused by upward-shift of atomic density distribution among metal line.

References

[1] e.g. C.S. Hau-Riege, *Microelectronics Reliability*, ol.44(2004), pp.195-205.

[2] K. Sasagawa, et al., *Proc. of 12th EMAP*, *EMAP*(2010), 230, 110-116.

[3] K. Sasagawa, M. Hasegawa, M. Saka, and H. Abé, *Journal of Applied Physics*, Vol. 91, 2002, pp.1882-1890.

[4] M. H. Lin, K. P. Chang, K. C. Su and T. Wang, *Microelectronics Reliability*, Vol.47, (2007), pp.2100-2108.

[5] C. -K. Hu, R. Rosenberg, and K. Y. Lee, *Applied Physics Letters*, Vol.74, Iss.20 (1999), pp.2945-2947.

[6] K. Sasagawa, M. Hasegawa, Saka, M. and Abé, H., *Journal of Applied Physics*, Vol.91, (2002), pp.1882-1890.

[7] M. Hasegawa, et al., Proc. of IPACK'03 (CD-ROM), ASME (2003), IPACK2003-35064.